



# Multi-objective optimization on the machining parameters for bio-inspired nanocoolant

K. Anamalai<sup>1</sup> · L. Samylingam<sup>1</sup> · K. Kadirgama<sup>1</sup> · M. Samykano<sup>1</sup> · G. Najafi<sup>2</sup> · D. Ramasamy<sup>1</sup> · M. M. Rahman<sup>1</sup>

Received: 18 June 2018 / Accepted: 17 August 2018 / Published online: 27 August 2018  
© Akadémiai Kiadó, Budapest, Hungary 2018

## Abstract

The emphasis of this paper is to evaluate the thermophysical properties of crystalline nanocellulose (CNC)-based nanofluid and the optimized machining parameters (cutting speed, feed rate and depth of cut) for machining using CNC-based nanofluid. Cutting tool temperature and formed chip temperature during machining are determined with CNC-based coolant and metal working fluid. Minimum quantity lubrication technique is used to minimize the usage of the coolant. Nanocellulose coolant with a concentration of 0.5% shows better thermal conductivity and viscosity. Total heat produced at the cutting tool and the temperature generated at the chip during machining shows significant improvement using CNC-based nanofluid. Statistical analysis reveals that feed rate and depth of cut contribute around 27.48% and 22.66% toward cutting temperature. Meanwhile, none of the parameters significantly affects the heat transfer. The multi-objective optimization reveals that the optimum parameter for machining using CNC-based nanocoolant is: cutting speed = 120, feed rate = 0.05 and depth of cut = 1.78 which produces heat transfer of 379.44 J and cutting temperature of 104.41 °C.

**Keywords** Nanocellulose · Multi-objective · Wear rate · Wear mechanism

## Introduction

The quest for energy has been humanity target since early ages. These craze has led the nature to be discarded and vandalized that has led to various environmental problems. As a remedy, various strategies and efforts are taken to preserve and reduce the problem. In the industrial world, machining is one of the key production processes [1, 2]. Machining is the most useful manufacturing process as the anticipated size, shape and surface finish are attained by removing the unwanted materials [3, 4]. The essential components in machining are the cutting tool and machine tool [5]. The cutting tool acts as a cutter where it eradicates the unwanted materials through chipping, whereas machine tool provides the required motion for the machining process to take place [6, 7]. During the operation, the contact

between tool and workpiece generates high heat due to the increased temperature. The temperature increases as the cutting speed is increased, causing a decrease in tool strength which leads to quicker wear and tool failure [8–10]. Also, the high heat generated at the cutting zone can result in a decreasing tool sharpness which leads to poor surface finish and increase in power consumption [10, 11]. Therefore, it is crucial to minimize the heat generated during machining to improve the product quality and cutting device life as found by Sarkaya and Güllü [12]. One of the possible mechanisms to reduce the heat generated is using cutting or cooling fluid [13, 14]. The primary responsibility of the cutting liquid is to banish the heat produced during the cutting contact between the workpiece and cutting tool [15, 16]. Lowering the heat helps in reducing the contact force during machining and eventually increases their life expectancy. The increase in the temperature during machining is typically instigated by chip formation and the friction force between the cutting tool and workpiece [17]. The high thermal load and friction force could also cause the cutter to wear quickly particularly at the tip of the cutting tool [18, 19]. The worn cutter

✉ K. Anamalai  
kumaran@ump.edu.my; maran717@yahoo.com

<sup>1</sup> Faculty of Mechanical Engineering, Universiti Malaysia Pahang, 26600 Pekan, Pahang, Malaysia

<sup>2</sup> Tarbiat Modares University, Tehran, Iran

would result in the deprived surface finish and poor dimensional accurateness. Where else, the use of cutting fluid promotes the development of built-up edge (BUE) and buildup layer (BUL) which also damages the surface of the workpiece [14, 20]. Nevertheless, cutting fluid helps not only to reduce the heat but also to remove the chips produced while machining [21, 22]. However, cutting fluid can possess significant environmental problems due to their hazardous chemical contents. In USA, ILMA (Independent Lubricant Manufacturers Association) reported about 95–103 mil gallons of coolants is disposed off yearly [19, 23]. The high amount of disposal is due to the traditional flood cooling technique which uses high amount of MWF. The use of enormous amount of cutting liquid causes natural issues such as water contamination, air contamination, the barrenness of the plant. Apart from that, machine administrators exposure to this liquid causes significant health issues such as skin disease and respiratory issues [24, 25]. All the problems triggered by existing flood coolant machining have urged researchers to reconnoiter ways to minimize the quantity of MWF used in machining. Minimum quantity lubrication (MQL) has been identified as one of the most feasible replacements for current flood machining system [26]. MQL system supplies the coolant in the mist that is focused straight to the cutting zone interface [27, 28]. Since a very small quantity of liquid is used, improved and superior heat-carrying capacity cutting fluids are required. As such, nanofluids are identified to be the best candidate to fulfill these expectations [29, 30]. Nanofluids are a composite of fluids in which the base fluid is suspended with either metallic or nonmetallic nanoparticles [31, 32]. These novel fluids have superior thermophysical properties and heat transfer performance compared to conventional fluids [35, 36]. Findings from previous studies related to nanofluids containing nanoparticles such as  $\text{TiO}_2$  and  $\text{SiO}_2$  showed superior performance and promising candidate for MWF replacement in MQL technique [33]. Since the ultimate goal is to develop cheaper, compelling and environmental-friendly fluid for MQL system, it is preferred naturally based nanomaterials instead using  $\text{SiO}_2$  or  $\text{TiO}_2$  nanoparticles. As such, CNC extricated from plants particularly from Canadian Hemlock tree is expected to be the best contender. Till date, there is no reported previous research on utilizing CNC-based nanofluid coolant for the machining operation. CNC-based nanofluid is reported to be chemically stable which is appropriate to be used for thermal transport applications [34]. Besides, the CNC also reported to have hydrophilic characteristics that helps in even dispersion in base fluid [35].

Response surface methodology (RSM) is a statistical analysis technique used to build an empirical model. RSM is initially used to model the experimental responses and later in modeling the numerical experiments. The basis for

this model is the developed DOE, where the response or output variable is optimized through several independent variables (input variables). The changes are made in experimental tests (runs) to identify the explanations for the variations in the output response. In physical experiments, the imprecision is believed due to errors in the measurement. In computer-based simulation or modeling experiments, the errors are known to be due to the improper convergence between iterative stages, round-off error and the discrete continuous physical phenomena. The errors are presumed to be random.

RSM is a methodology of estimating the approximations of the system behavior using findings obtained in the response analyses calculated from series of points in the variable space. Usually, the RSM optimization can be unraveled following three stages: (a) DOE, (b) model building and (c) solution of minimization problem conferring to the criterion selected. RSM is a blend of experimental, regression study and statistical inferences. The base idea of an RSM is to include all the variables known as a dependent variable,  $y$ , and several other independent variables,  $x_1, x_2, \dots, x_k$ . By assuming all the variables is measurable, the response surface can be expressed as,  $y = f(x_1; x_2; \dots; x_k)$ .

Since the ultimate goal is to optimize the response of variable  $y$ , the independent variables are assumed to be random, continuous and controllable by the experimenter with insignificant error (negligible). For instance, in a turning machining operation, it is required to find the appropriate combination of cutting speed ( $x_1 = \ln V$ ), feed rate ( $x_2 = \ln f$ ) and depth of cut ( $x_3 = \ln a$ ) to enhance the response. The response  $y$  as a function of speed, feed rate and depth of cut can be expressed as,  $y = f(x_1, x_2, x_3) + \varepsilon$ .

Generally, a low-order polynomial (first-order and second-order) is used in certain regions of the independent variables. The first-order model is as follows:

$$y = \beta_0 + \sum_{i=1}^k \beta_i x_i + \varepsilon$$

The second-order model as follows:

$$\sum_{i=1}^k \beta_i x_i + \sum_{i=1}^k \beta_{ij} x_i^2 + \sum_i \sum_j \beta_{ij} x_i x_j + \varepsilon \text{ for } i < j$$

The RSM is easy, economical and practical to be used in modeling machining processes.

Hill and Hunter [36] have studied the initial works performed using RSM. They summarized that to establish an excellent functional association between the surface roughness and cutting parameters (speed, depth of cut and feeds), a great number of experiments are needed in which it requires a discrete set of trials for each experimental combination. By using factors such as cutting speed, feed

and the side cutting edge angle (SCEA), Noordin et al. [37] have described the performance of a multilayer tungsten carbide tool. They reported that the “feed” is the most significant factor that affects the surface roughness. Also, Neşeli et al. [38] have investigated the tool geometry influence on the surface roughness of machined AISI 1040 steel using RSM. They reported that RSM method has a good agreement with the measured surface roughness. They also proved that the developed RSM model could be used to predict the surface roughness AISI 1040 steel.

## Materials and methods

### Preparation of nanofluid

Crystalline nanocellulose (CNC) has been material of interest in numerous applications, mainly as a filler in bio-composites. The sustainability, environmental-friendly, excellent mechanical properties, high flexibility and good thermal and electrical properties are some advantageous characteristics of nanocellulose [39]. The acquired CNC for this work was supplied by Blue Goose Biorefineries Inc. which was extracted from Western Hemlock plant. As the purchased CNC is in mass%, the nanofluid was prepared by dilution method adopting two-step method. The nanofluid is prepared by dispersing CNC in EG (ethylene glycol)–W (distilled water) mixture. Initially, the mass concentration,  $\omega$ , is converted to volume concentration,  $\phi$ , by using Eq. (1). Then, the CNC is dispersed in base fluid (40% EG and 60% W),  $\Delta V$ , at preferred concentration,  $\phi_2$ , which determined using Eq. (2), followed by stirring by using magnetic stirrer for 30 min. Finally, the prepared solution is ultrasonicated for 2 h by using Fisher brand model number FB1505 to produce a stable and homogeneous nanofluid. Table 1 lists the CNC specification as provided by the provider.

$$\phi = \omega \rho_w / (1 - \omega / 100) \rho_p + (\omega / 100) \rho_w \quad (1)$$

$$V_1 (\phi_1 / \phi_2 - 1) \quad (2)$$

### Measurement of thermal conductivity

The size, shape and type of nanoparticles used are shown to influence the thermal conductivity of the nanofluids [40].

**Table 1** CNC specification

Specification	Value
Index of crystallinity	80%
Length of crystal length	100–150 nm
Diameter of crystal	9–14 nm

For instance, nanofluid containing nonmetal nanoparticles reported having inferior thermal conductivity properties compared to those having metal nanoparticles, whereas, nanofluid with smaller particle sizes has superior thermal conductivity properties [41]. Also, the shape of the nanoparticle also influences the thermal conductivity; cylindrically shaped nanoparticles exhibit more excellent thermal conductivity compared to nanoparticles with spherical shape [42]. KD2 Pro Thermal Property Analyser (Decagon Devices, Inc., USA) is used in this work to investigate the thermal behavior of the prepared nanofluid. This analyzer comprises a controller and KS-1 (60 mm) sensors that are used to measure the thermal properties. The measurement was taken at a temperature between 30 and 70 °C (controlled condition). Memmert water bath (with an accuracy of 0.1 °C) is used to regulate the temperature. Prior to the actual experiments, the KD2 pro is validated by determining the thermal conductivity of benchmark solution supplied by the equipment manufacturer (glycerin,  $k = 0.285 \text{ W m}^{-1} \text{ K}^{-1}$  at 20 °C) solution. Also, the measurement is further authenticated by measuring the base fluid thermal conductivity (40% EG and 60% W) and compared with the predetermined values from ASHRAE (American Society of Heating, Refrigerating and Air-Conditioning Engineers). The comparison shows a very small maximum deviation of about 1.4% between the base fluid and ASHRAE data. These affirm the ability and reliability of the equipment in performing the measurement. The actual measurement was taken for 20 readings at 15-min interval for each sample concentration and averaged to minimize the experimental error.

### Measurement of dynamic viscosity

Dynamic viscosity is measured by measuring the viscous drag created by the spindle rotation on Brookfield LVDV-III Rheometer. The data are collected using a personal computer which connected to the rheometer. A minimum of five (5) readings are obtained from each concentration and averaged to minimize the error and to obtain an accurate data. The collected data show the maximum deviation of 12.19% upon compared with ASHRAE data. Prior to the actual nanofluid viscosity measurement, the rheometer ability is validated. The validation was carried out by measuring the base fluid (containing 40% EG and 60% W) and compared with the value obtained from predetermined ASHRAE values. The measurement is taken once a good covenant is obtained between actual and the modeled values.

### Turning machining operation

In this present work, minimum quantity lubrication (MQL) technique is espoused by using the Unist Coolubricator

with a storage capacity of 1893 mL cutting fluid. This storage functions with the supply of electrical power and compressed air. A flow rate of 10 mL per hour (constant for all experiments) is used by regulating pulse generator knob on the Unist Coolubricator. The Unist Coolubricator nozzle is pointed appropriately to the tool and workpiece contact location for precise cutting fluid deliverance and cooling.

Ceratizit material-based tool bit with the ISP catalog number of TPUN 160304EN is used in this study, whereas the turning insert used in this work is the tungsten–cobalt (cemented WC–Co) CVD coated with Ti (C,N) + Al<sub>2</sub>O<sub>3</sub>. The total thickness of the coating is 15 μm. The insert with Ti (C,N) + Al<sub>2</sub>O<sub>3</sub> coating is chosen as this insert has high wear resistant and helps toward reducing the friction. Figure 1 displays the SEM image of the cutting tool inner layers. It is also expected that this coating has a good metallurgical bond with the cutting tool for better wear properties. A triangular-shaped insert is used together with a tool holder. The insert is replaced for each experimental parameter studied. The insert specification is as follows:  $d = 9.525$  mm,  $l = 16.51$  mm,  $s = 3.175$  mm,  $r = 0.406$  mm, mass of the cutting tool = 0.01 kg, and the specific heat capacity is  $945 \text{ J kg}^{-1} \text{ }^\circ\text{C}^{-1}$ .

In this investigation, the SUS 304 stainless steel rod is used as the workpiece material with a diameter of 32 mm and length of 120 mm. The Rockwell hardness value for this rod is around B 103. Meanwhile, the chemical composition of the SUS 304 stainless steel rod is determined using the method of mass spectrometry. Table 2 lists the chemical compositions of the SUS 304 stainless steel determined by the method of mass spectroscopy, whereas Table 3 shows the physical properties of workpiece material (SUS 304 Stainless steel).

There are two separate investigations performed in this work. In the first study, the machining operation (lathe) of

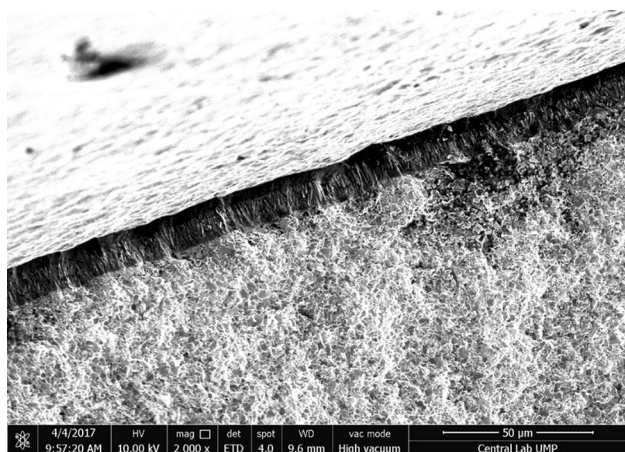


Fig. 1 SEM image of the cutting tool inner layers

stainless steel (SUS 304) was performed using MWF. While in the second study, the machining operation was carried out using CNC-based coolant. The machining parameter used for both is similar and shown in Table 4. The varied parameter such as cutting speeds was set to be  $120 \text{ m min}^{-1}$  and  $160 \text{ m min}^{-1}$ , the depths of cut was set to be 0.5–2.0 mm, and the feed rate was set to be  $0.05\text{--}0.15 \text{ mm rev}^{-1}$ . The experiment setup for the present work is shown in Fig. 2.

Also in this study, an infrared (IR) sensitive thermometer was used to evaluate the thermal energy generated during the machining process. The critical parameter which needs to be determined before evaluating the thermal radiation using this method is the emissivity. The emissivity used for measuring the chip temperature for an “ongoing” machining operation is 0.85, whereas the emissivity used for measuring the cutting tool temperature is set to be 0.05. The purpose of measuring this temperature is to estimate the heat generated at the cutting tool during the machining process. The measurement is taken on both workpiece and cutting tool. Also, the temperature generated at the chip formed during machining was also measured and analyzed. These are to have a clear perspective on the heat conveyance during the machining operation. The overall flow of the work done for the analysis is shown in Fig. 3.

## Results and discussion

### Nanofluid stability evaluation and analysis

The liquid stability is assessed via sedimentation observation (qualitative technique) as shown in Fig. 3. The steadiness of the nanofluid is essential for stable transportation of heat exchange and to avoid sedimentation in the storage tank. The observation (Fig. 4) demonstrates no sedimentation of nanomaterial occurred at the bottom of test tube even after over a month which proved nanofluid’s high dependability.

### Nanofluid thermal conductivity evaluation and analysis

Initially, the thermal conductivity measurement is validated for base fluid at the composition 40:60 EG/W and compared with ASHRAE. Later, the nanofluid is prepared at a volume concentration of 0.1%, 0.5%, 0.9% and 1.3% and their thermal conductivity is estimated. Finally, the thermal conductivity measurement is also taken for metal working fluid, MWF) at the proportion of 40% MWF and 60% distilled water. All the measurement is taken at three particular temperatures which is  $30 \text{ }^\circ\text{C}$ ,  $50 \text{ }^\circ\text{C}$  and  $70 \text{ }^\circ\text{C}$ .



**Table 2** Chemical elements in SUS 304 stainless steel

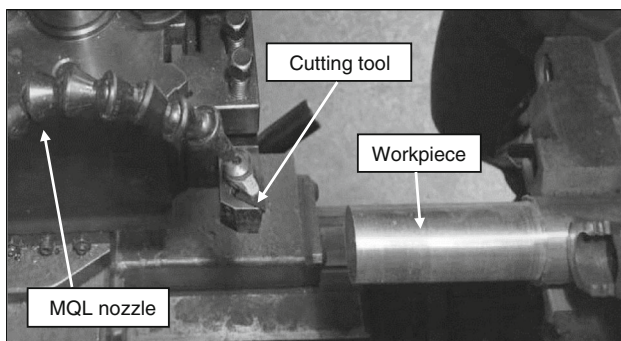
Component	FE	CR	NI	MN	SI	CU	MO	CO	C
Mass/%	70.20	17.80	8.32	1.44	0.62	0.56	0.46	0.21	0.07

**Table 3** Physical properties of SUS 304 stainless steel

Properties	Value	Unit
Density	7880	kg m <sup>-3</sup>
Elastic modulus	193.0	GPa
Thermal expansion coefficient	0.0000174	°C <sup>-1</sup>
Thermal conductivity	15.1	at 100 °C
Thermal conductivity	19.4	at 500 °C
Specific heat	496	J kg <sup>-1</sup> K <sup>-1</sup>

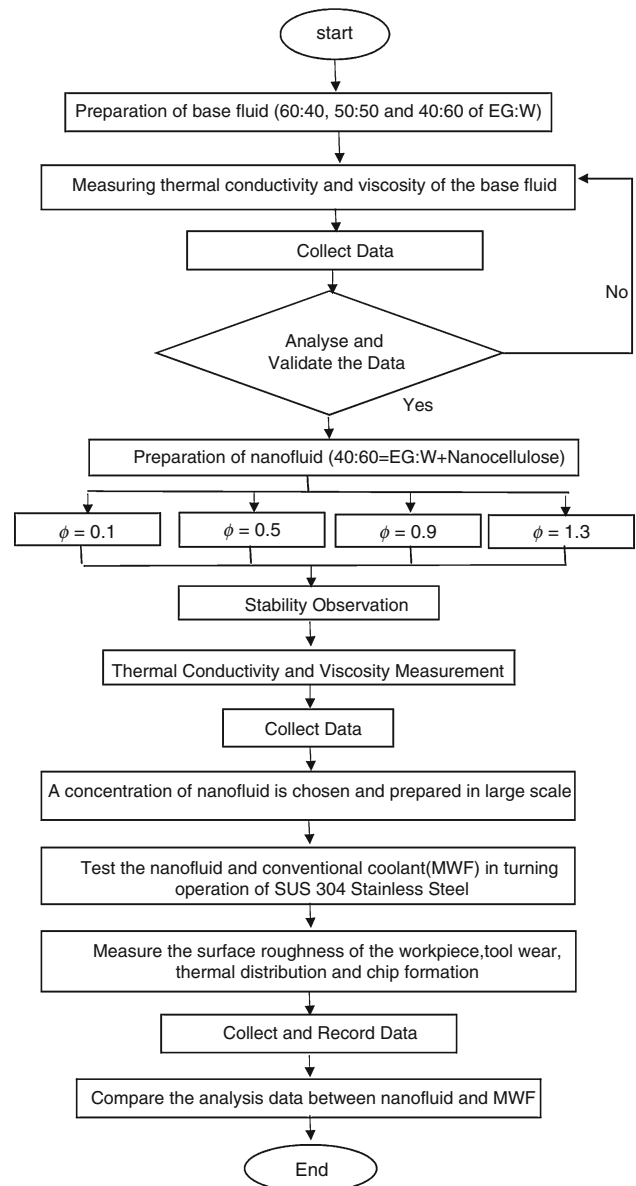
**Table 4** Variable values for the selected parameter

Factors	-1	0	1
Speed, $V_c/m \text{ min}^{-1}$	120	140	160
Feed rate, $F/mm \text{ rev}^{-1}$	0.05	0.10	0.15
Depth of cut, $D/mm^{-1}$	0.5	1.25	2.0

**Fig. 2** Machining setup using MQL

The measurement is taken for both coolants and analyzed to determine their viability. Figure 5 reveals the thermal conductivity finding for both MWF and nanocoolants at different volume concentrations.

The improvements in thermal conductivity with respect to temperature and volume concentrations are shown in Fig. 5. The highest enhancement in thermal conductivity is recorded at the temperature of 70 °C and volume concentration of 1.3%. Naik and Sundar [43] have also obtained the similar thermal behavior in their studies using ethylene glycol- and water blend-based Fe<sub>3</sub>O<sub>4</sub> nanofluid. The improved thermal behavior is believed due to the higher collision between particles at higher temperatures known as Brownian motion. Figure 5 also proves that the thermal

**Fig. 3** General work done on the fluid

conductivity of the developed nanofluid is much better than the MWF. Also, the figure demonstrates the ability of CNC-based nanofluid in assimilating the thermal energy produced during the machining particularly at the inter-phase of workpiece and cutting device compared to MWF. Roy et al. [44] have also encountered a similar finding using multi-walled carbon nanotube (MWCNT)-based nanofluid.

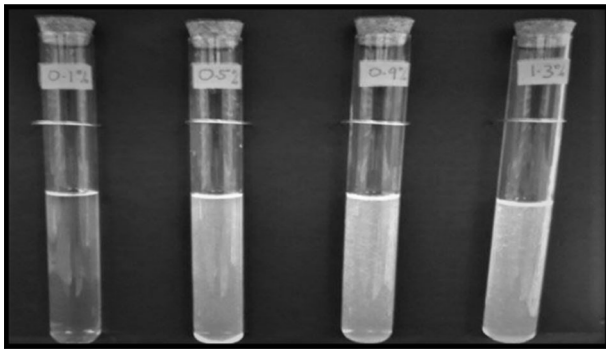


Fig. 4 Sedimentation observation after 1 month

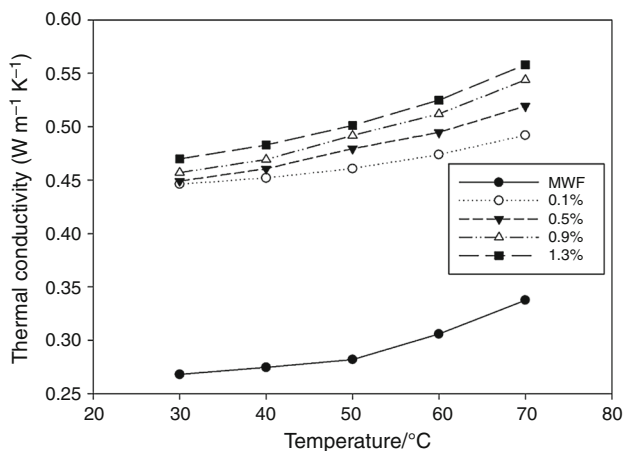


Fig. 5 Thermal conductivity of nanocoolants at various volume concentration

### Nanofluid dynamic viscosity evaluation and analysis

The volume concentration that has been evaluated for dynamic viscosity is 0.1%, 0.5%, 0.9% and 1.3%. The viscosity has been estimated for three particular temperatures which are 30 °C, 50 °C and 70 °C. Then, the consistency assessment is additionally done for MWF-W at the proportion of 40:60. The two-test information is obtained and analyzed to determine the viability of both coolants. Figure 6 shows the viscosity of CNC-based nanofluid at different volume concentration and MWF.

As can be seen from Fig. 6, the viscosity observed to decrease as the temperature is increased and increase as the volume concentration is increased. The highest viscous is recorded at the temperature of 30 °C and volume centralization of 1.3%, whereas the lowest viscous is recorded for nanofluid with volume concentrations 0.1% and temperature of 70 °C. The reduction in viscosity as the temperature increased is believed due to enhanced movement between atoms and particles at subatomic level [45]. Therefore, the free volume in the nanofluid structure will expand, and the

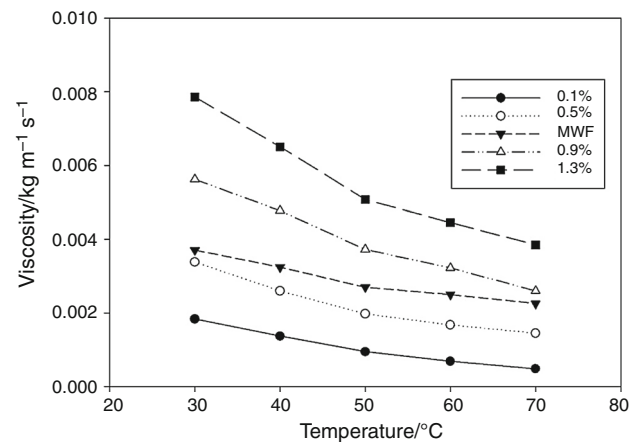


Fig. 6 Viscosity of nanofluid at various volume concentration and MWF

inner interaction powers between particle diminish. However, the increased viscosity as the volume concentration increase is expected to be due to the increased liquid interior shear pressure. The MWF, though, recorded to have a lower viscosity than the 0.9% and 1.3% volume concentrated CNC-based nanofluid, but higher than nanofluid with a concentration of 0.5% and 0.1%. In a machining operation, a low viscous coolant is preferred that high viscous to eliminate the lubricity effect and better energy utilization. As such, the nanofluid with a concentration of 0.5% and 0.1% would be the best choice to be used as a coolant.

### Selection of nanofluid composition

Based on the findings shown in Fig. 5, the nanofluid comprising CNC displays better thermal conductivity properties compared to MWF. However, the nanofluid with a volume concentration of 0.5% and 0.1% has the viscosity lower than MWF, which is required and best for machining. As such, by taking into account both properties and the required criteria (higher thermal properties and lower viscosity than MWF), the nanofluid with 0.5% volume concentration is selected. The selected nanofluid (0.5% volume concentration) is then utilized in the machining operation to determine its effectiveness and suitability to be used as coolant replacing MWF in a machining operation.

### Cutting tool thermal behavior

The removal of metal during machining work involves forces and friction which eventually transformed to heat at the interface of the cutting tool and workpiece [46]. In order to measure the nanofluid effectiveness in removing the heat generated at cutting tool, the temperature at the cutting tool is measured before and after an 80-mm length



Fig. 7 Cutting tool temperature measurement

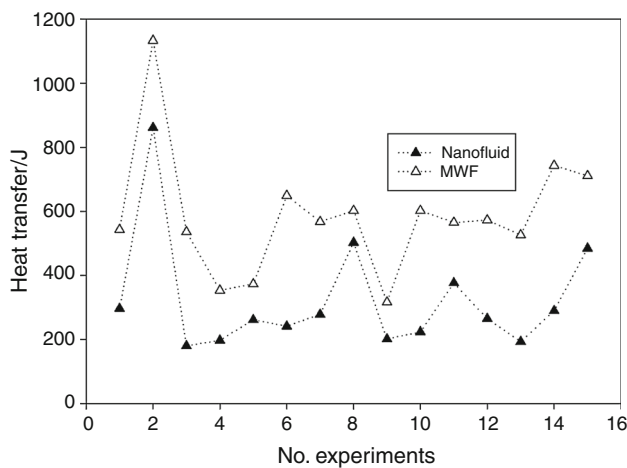


Fig. 8 Measured heat transfer for each experiment using nanofluid and MWF

of cut using CNC-based nanofluid and MWF. The infrared camera is also used to obtain the thermal image at the cutting tool during the experiment as shown in Fig. 7, whereas Fig. 8 displays the difference in heat transfer experienced by the cutting tool using CNC-based nanofluid and MWF coolant.

From Fig. 8, it is evident that the cutting tool experiences lower heat using CNC-based nanofluid compared to MWF. The highest heat energy recorded is 1130 J while using

MWF. Whereas the highest heat energy observed while using nanofluid is 863 J, the lowest heat energy recorded on MWF is 312 J and 196 J using CNC-based nanofluid. Also, the heat energy recorded while using MWF is 530 J and meanwhile 175 J using nanofluid. Thus, this undoubtedly proves that the CNC-based nanofluid has good heat transfer characteristics compared to MWF. As such, the nanofluid is capable of elimination of excess heat energy which is transferred to a cutting tool which in turn, improves the tool life. Also, the total heat energy produced at the workpiece is reduced. With the improved cooling performance, the surface roughness of workpiece is improved and the tool wear related to BUE is reduced. Yogeswaran et al. [37] state that no sticky surface or BUE or rough surface observed when nanofluid used in their investigations.

Analysis of variance (ANOVA) as shown in Table 5 is performed to examine the influence of the considered factors on the heat transfer capacity of the fluid. The evaluated factors are the cutting speed, feed rate and cutting depth. The output factor would be the heat transfer. The *p* value would determine the level of the impact, whether huge or small. If the impact is large, the resulting factor would be more than zero. If the figured *p* value is more noteworthy than the level of noteworthiness, then the impact of the factor is said to be small. The level of the significant is set to 0.05 to allow the chosen parameters with insignificant impact to be excluded [47]. From the analysis, none of the investigated factors seem to significantly affect the heat transfer behavior as shown in Fig. 9. The first-order equation to predict heat transfer is:

$$\text{Heat transfer (nano)} = 241 - 0.27 \text{ Cutting speed} + 14 \text{ feed rate} + 95.6 \text{ axial of depth} \tag{3}$$

The main effect plot shows that an increase in depth of cut increases the heat transfer as shown in Fig. 10. Figure 11 shows the predicted value from Eq. (3) compared with experimental values. The error is from 5 to 11%.

Table 5 ANOVA for heat transfer

Source	DF	Seq SS	Contribution/%	Adj SS	Adj MS	F value	p value
Model	3	41,368	9.26	41,368	13,789.2	0.37	0.773
Linear	3	41,368	9.26	41,368	13,789.2	0.37	0.773
Cutting speed	1	240	0.05	240	240.3	0.01	0.937
Feed rate	1	4	0.00	4	3.7	0	0.992
Axial of depth	1	41,124	9.20	41,124	41,123.7	1.12	0.314
Error	11	405,482	90.74	405,482	36,862		

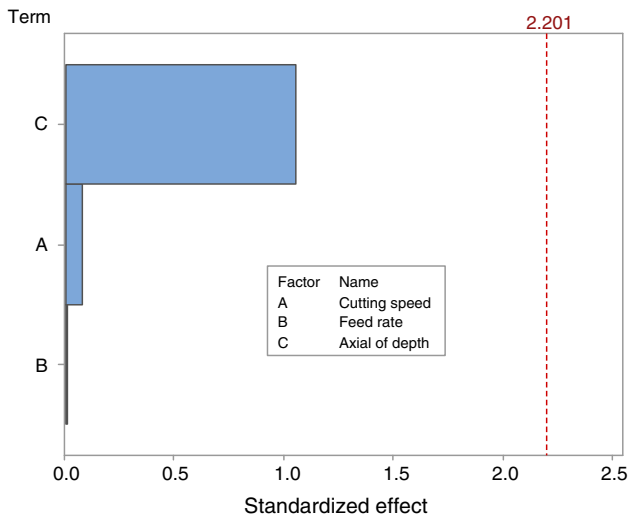


Fig. 9 Pareto chart for significant parameters

**Analysis of thermal distribution at the chip formation**

Heat distribution analysis is further performed on the chip formed during machining using the CNC-based nanofluid and conventional fluid. The heat distribution image is taken after a specific length of cut (50 mm) for each cutting parameter examined. The image showing the measured temperature at the chip during machining is shown in Fig. 12. The same procedure as shown in Fig. 12 is used to measure the chip temperature for all other parameters using the nanofluid and MWF. From all the measured temperature (Fig. 13), it is evident that the heat generated at chip using nanofluid is significantly less than using MWF. The highest recorded temperature using nanofluid was 154 °C

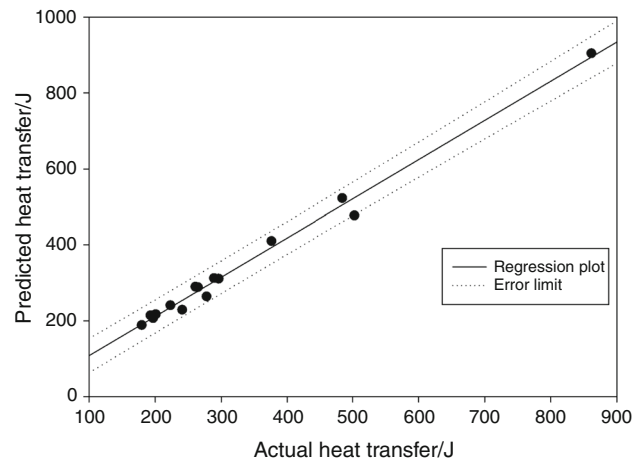


Fig. 11 Comparison between actual and predicted values

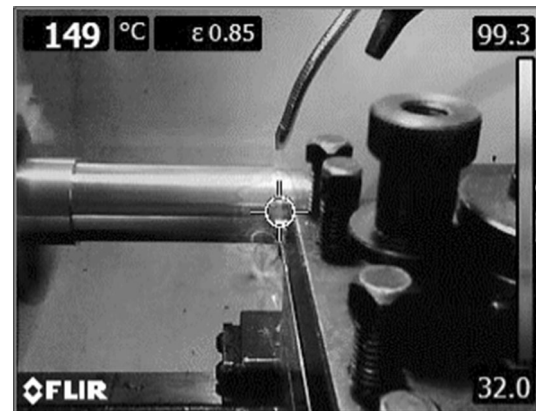
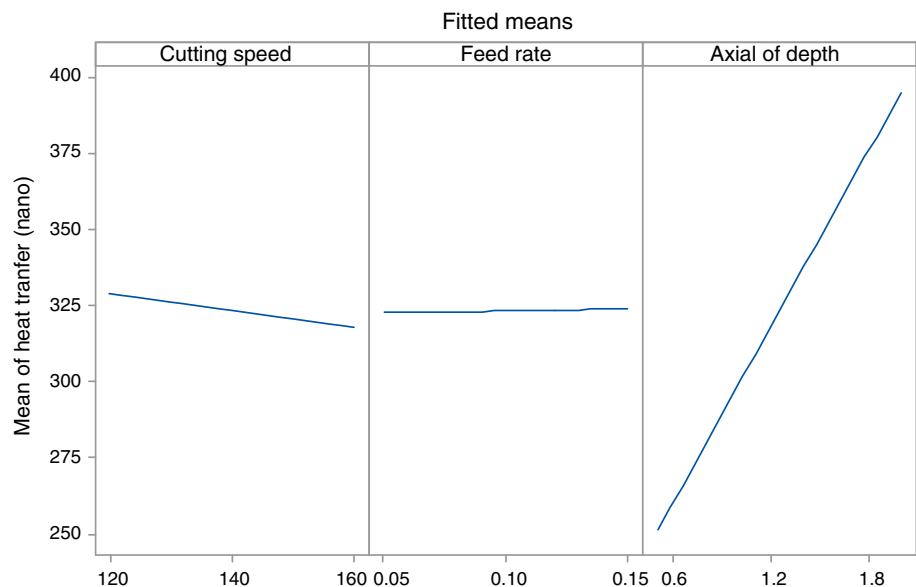


Fig. 12 Temperature at the chip (cutting length 50 mm) using MWF

Fig. 10 Factorial plot





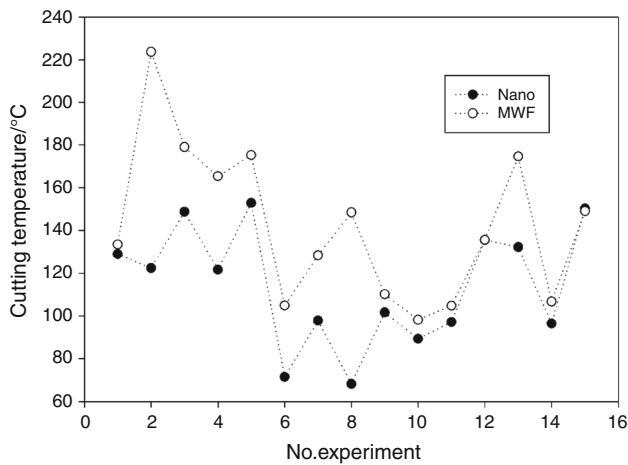


Fig. 13 Measured temperature for each experiment using nanofluid and MWF

while for MWF was 225 °C, whereas the lowest recorded temperature for nanofluid was 67.3 °C and MWF was 98 °C. The observed reduction in temperature at the formed chip during machining is attributed to the higher thermal conductivity properties of the CNC-based nanofluid.

Analysis of variance (ANOVA) as shown in Table 6 is performed to examine the influence of the considered factors on the heat transfer capacity of the fluid. The evaluated factors are the cutting speed, feed rate and cutting depth. The output factor would be the heat transfer. The *p* value would determine the level of the impact, whether huge or small. If the impact is large, the resulting factor would be more than zero. If the figured *p* value is more noteworthy than the level of noteworthiness, then the impact of the factor is said to be small. The level of the significant is set to 0.05 to allow the chosen parameters with insignificant impact to be excluded [47]. From the performed analysis, the feed rate and depth of cut found to significantly affect the cutting temperature, as shown in Fig. 14. Feed rate contributes around 27.48% and depth of cut around 22.66%. As such, the feed rate is the primary

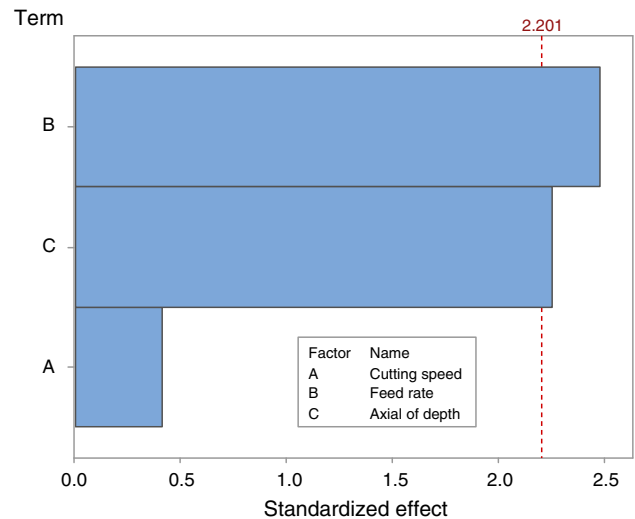


Fig. 14 Pareto chart for the factor analysis

factor which affects the cutting temperature. The first-order equation to predict temperature is:

$$\text{Temperature} = 24.6 + 0.159 \text{ Cutting speed} + 384 \text{ feed rate} + 23.2 \text{ axial of depth} \tag{4}$$

The main effect plot shows that an increase in depth of cut and feed rate increases the cutting temperature as shown in Fig. 15. Figure 16 shows the predicted value from Eq. (4) compared to experimental values. The error is from 7 to 14%.

### Multi-objective optimization

The machining parameters need to be optimized with three properties so that it will indicate the optimum parameters (cutting speed, feed rate and depth of cut) for heat transfer and cutting temperature. Sarıkaya and Güllü [12] also used this technique to optimize Haynes 22. The optimization criteria were selected to be maximum heat transfer and minimum cutting temperature. The optimization produces

Table 6 ANOVA for cutting temperature

Source	DF	Seq SS	Contribution/%	Adj SS	Adj MS	F value	p value
Model	3	5448.2	50.89	5448.24	1816.08	3.80	0.043
Linear	3	5448.2	50.89	5448.24	1816.08	3.80	0.043
Cutting speed	1	81.0	0.76	81.01	81.01	0.17	0.688
Feed rate	1	2941.7	27.48	2941.74	2941.74	6.16	0.031
Axial of depth	1	2425.5	22.66	2425.48	2425.48	5.08	0.046
Error	11	5257.2	49.11	5257.20	477.93		
Lack-of-fit	9	4581.2	42.79	4581.22	509.02	1.51	0.462
Pure error	2	676.0	6.31	675.97	337.99		
Total	14	10,705.4	100.00				

**Fig. 15** Factorial analysis for cutting temperature

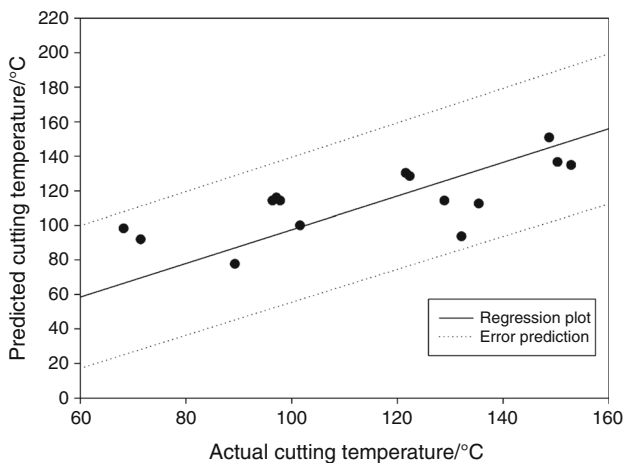
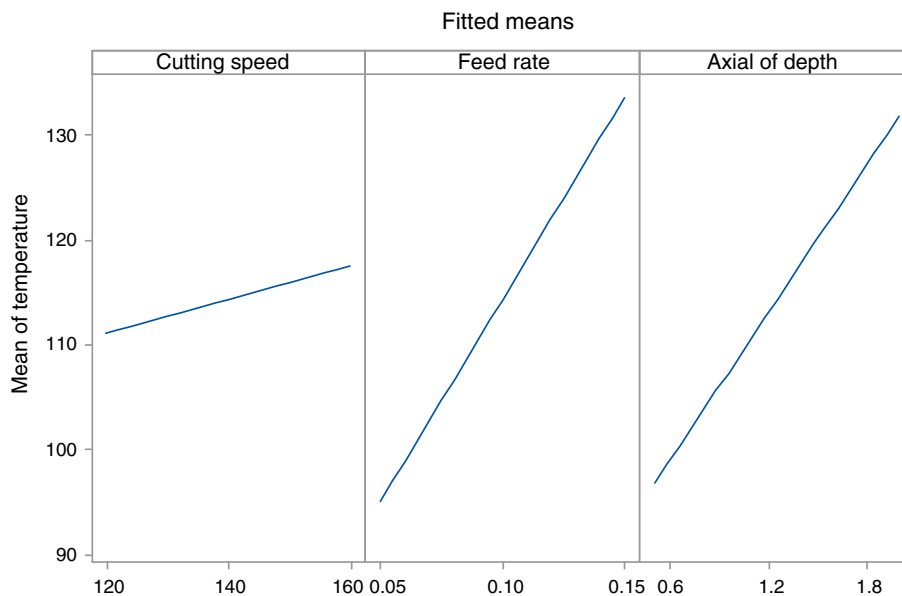


**Fig. 16** Comparison between actual and predicted values

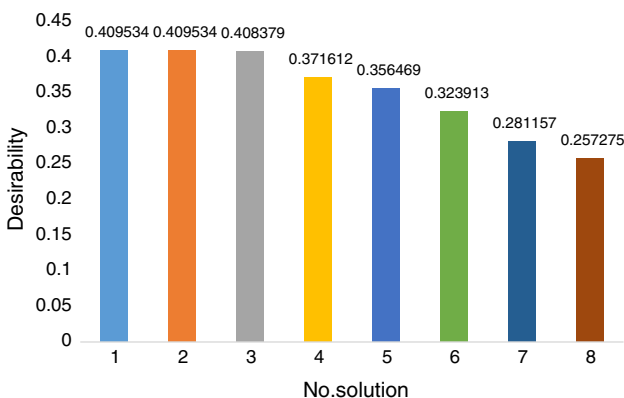


**Fig. 17** Solution for the multi-objective

eight (8) solutions that meet with the criteria with different desirability as shown in Fig. 17. It shows that the first solution produces the optimum parameters to produce maximum heat transfer and minimum cutting temperature. The optimum parameters are cutting speed = 120, feed rate = 0.05 and depth of cut = 1.78 which produces heat transfer = 379.44 J and cutting temperature = 104.41 °C.

### Conclusions

In this work, the effectiveness of CNC-based nanofluid coolant is studied, optimized and proved to perform better than the MWF using MQL coolant system. The summary of the significant findings is as follows:

- Total heat generated at the cutting tool using CNC-based nanofluid is significantly lower compared to the heat generated by using MWF.
- CNC-based nanofluid observed to have a high thermal conductivity which enables efficient heat transfer ability which improves the tool life.
- The machining operation using the selected nanofluid concentration (0.5%) shown to have a superior thermal conductivity (0.449 W m<sup>-1</sup> K<sup>-1</sup>) than conventional MWF (0.267 W m<sup>-1</sup> K<sup>-1</sup>) at 30 °C. The obtained heat transfer at cutting tool using MWF was 1130 J, while CNC-based nanofluid was 863 J, significantly lower.
- The statistical method reveals that the feed rate and axial depth of cut contribute around 27.48% and 22.66% toward cutting temperature. Meanwhile, none of the parameters significantly affect the heat transfer.

- The prediction Eqs. (3) and (4) produce error around 5–14% compared with the experimental values.
- The multi-objective optimization provides the optimized parameters for machining: cutting speed = 120, feed rate = 0.05 and axial depth of cut = 1.78, which produces heat transfer = 379.44 J and cutting temperature = 104.41 °C.

**Acknowledgements** The authors would like to thank the Minister of Higher Education for providing Grant under the Fundamental Research Grant Scheme (FRGS) RDU130129, RDU180328 and Universiti Malaysia Pahang for providing facilities to conduct the research.

## References

1. Davim JP. *Machining: fundamentals and recent advances*. Berlin: Springer; 2008.
2. Mia M, et al. Influence of Ranque–Hilsch vortex Tube and nitrogen gas assisted MQL in precision turning of Al 6061-T6. *Precis Eng*. 2018;53:289–99.
3. Shaw M, Vyas A. Chip formation in the machining of hardened steel. *CIRP Ann Manuf Technol*. 1993;42(1):29–33.
4. Mia M, et al. An approach to cleaner production for machining hardened steel using different cooling-lubrication conditions. *J Clean Prod*. 2018;187:1069–81.
5. Gupta MK, Sood P. Surface roughness measurements in NFMQL assisted turning of titanium alloys: an optimization approach. *Friction*. 2017;5(2):155–70.
6. Puvanesan M, et al. Experimental investigation of minimum quantity lubrication on tool wear in aluminum alloy 6061-t6 using different cutting tools. *Int J Autom Mech Eng*. 2014;9:1538.
7. Razak N, Rahman M, Kadirgama K. Investigation of machined surface in end-milling operation of hastelloy c-2000 using uncoated-carbide insert. *Adv Sci Lett*. 2012;13(1):300–5.
8. Altin A, Nalbant M, Taskesen A. The effects of cutting speed on tool wear and tool life when machining Inconel 718 with ceramic tools. *Mater Des*. 2007;28(9):2518–22.
9. Kadirgama K, et al. Tool life and wear mechanism when machining Hastelloy C-22HS. *Wear*. 2011;270(3):258–68.
10. Kadirgama K, et al. Aspects of wear mechanisms of carbide tools when machine Hastelloy C-22HS. In: *Advanced materials research*. Trans Tech Publications; 2010.
11. Gupta MK, Sood P. Machining comparison of aerospace materials considering minimum quantity cutting fluid: a clean and green approach. *Proc Inst Mech Eng Part C J Mech Eng Sci*. 2017;231(8):1445–64.
12. Sarkaya M, Güllü A. Multi-response optimization of minimum quantity lubrication parameters using Taguchi-based grey relational analysis in turning of difficult-to-cut alloy Haynes 25. *J Clean Prod*. 2015;91:347–57.
13. Muthukrishnan N, Davim P. Influence of coolant in machinability of titanium alloy (Ti-6Al-4V). *J Surf Eng Mater Adv Technol*. 2011;1(1):9–14.
14. Jayal AD, Balaji A. Effects of cutting fluid application on tool wear in machining: interactions with tool-coatings and tool surface features. *Wear*. 2009;267(9):1723–30.
15. Najiha M, Rahman M, Kadirgama K. Performance of water-based TiO<sub>2</sub> nanofluid during the minimum quantity lubrication machining of aluminium alloy, AA6061-T6. *J Clean Prod*. 2016;135:1623–36.
16. De Chiffre L, Belluco W. Investigations of cutting fluid performance using different machining operations. *Tribol Lubr Technol*. 2002;58(10):22.
17. Muthusamy Y, et al. Wear analysis when machining AISI 304 with ethylene glycol/TiO<sub>2</sub> nanoparticle-based coolant. *Int J Adv Manuf Technol*. 2016;82(1–4):327–40.
18. Schuldt S, et al. Analysis of the sharpness of blades for food cutting. *J Food Eng*. 2016;188:13–20.
19. Gupta MK, Sood P, Sharma VS. Optimization of machining parameters and cutting fluids during nano-fluid based minimum quantity lubrication turning of titanium alloy by using evolutionary techniques. *J Clean Prod*. 2016;135:1276–88.
20. Najiha M, Rahman M, Kadirgama K. Machining performance of aluminum alloy 6061-T6 on surface finish using minimum quantity lubrication. *Int J Autom Mech Eng*. 2015;11:2699.
21. Avila R, Abrao A. The effect of cutting fluids on the machining of hardened AISI 4340 steel. *J Mater Process Technol*. 2001;119(1):21–6.
22. Mia M, Dhar NR. Influence of single and dual cryogenic jets on machinability characteristics in turning of Ti–6Al–4V. *Proc Inst Mech Eng Part B J Eng Manuf*. 2017; 10.1177/0954405417737581.
23. Mia M, Dhar NR. Effects of duplex jets high-pressure coolant on machining temperature and machinability of Ti–6Al–4V superalloy. *J Mater Process Technol*. 2018;252:688–96.
24. Lawal S, Choudhury I, Nukman Y. Application of vegetable oil-based metalworking fluids in machining ferrous metals—a review. *Int J Mach Tools Manuf*. 2012;52(1):1–12.
25. Gupta K, Laubscher RF. Sustainable machining of titanium alloys: a critical review. *Proc Inst Mech Eng Part B J Eng Manuf*. 2017;231(14):2543–60.
26. Sarkaya M, Yılmaz V, Güllü A. Analysis of cutting parameters and cooling/lubrication methods for sustainable machining in turning of Haynes 25 superalloy. *J Clean Prod*. 2016;133:172–81.
27. Najiha M, et al. Multi-objective optimization of minimum quantity lubrication in end milling of aluminum alloy AA6061T6. *Int J Autom Mech Eng*. 2015;12:3003.
28. Dhar N, et al. The influence of minimum quantity of lubrication (MQL) on cutting temperature, chip and dimensional accuracy in turning AISI-1040 steel. *J Mater Process Technol*. 2006;171(1):93–9.
29. Lee P-H, et al. An experimental study on micro-grinding process with nanofluid minimum quantity lubrication (MQL). *Int J Precis Eng Manuf*. 2012;13(3):331–8.
30. Khandekar S, et al. Nano-cutting fluid for enhancement of metal cutting performance. *Mater Manuf Process*. 2012;27(9):963–7.
31. Ramachandran K, et al. Thermophysical properties measurement of nano cellulose in ethylene glycol/water. *Appl Therm Eng*. 2017;123:1158–65.
32. Yu W, et al. Review and comparison of nanofluid thermal conductivity and heat transfer enhancements. *Heat Transf Eng*. 2008;29(5):432–60.
33. Yogeswaran M, et al. Temperature analysis when using ethylene-glycol-based TiO<sub>2</sub> as a new coolant for milling. *Int J Autom Mech Eng*. 2015;11:2272.
34. Contreras J, Rodriguez E, Taha-Tijerina J. Nanotechnology applications for electrical transformers—a review. *Electr Power Syst Res*. 2017;143:573–84.
35. Morais JPS, et al. Extraction and characterization of nanocellulose structures from raw cotton linter. *Carbohydr Polym*. 2013;91(1):229–35.
36. Hill WJ, Hunter WG. A review of response surface methodology: a literature survey. *Technometrics*. 1966;8(4):571–90.

37. Noordin MY, Venkatesh VC, Sharif S, Elting S, Abdullah A. Application of response surface methodology in describing the performance of coated carbide tools when turning AISI 1045 steel. *J Mater Process Technol.* 2004;145(1):46–58.
38. Neşeli S, Yıldız S, Türkeş E. Optimization of tool geometry parameters for turning operations based on the response surface methodology. *Measurement.* 2011;44(3):580–7.
39. Thirivikraman G, et al. Nanomaterials in 3D bioprinting: current approaches and future possibilities. *Nanotechnol Prev Regener Med Emerg Big Picture.* 2017;47:349.
40. Esfe MH, et al. Experimental study on thermal conductivity of ethylene glycol based nanofluids containing  $Al_2O_3$  nanoparticles. *Int J Heat Mass Transf.* 2015;88:728–34.
41. Mehrali M, et al. Investigation of thermal conductivity and rheological properties of nanofluids containing graphene nanoplatelets. *Nanoscale Res Lett.* 2014;9(1):15.
42. Murshed SMS, Leong KC, Yang C. Investigations of thermal conductivity and viscosity of nanofluids. *Int J Therm Sci.* 2008;47(5):560–8.
43. Naik MT, Sundar LS. Investigation into thermophysical properties of glycol based CuO nanofluid for heat transfer applications. *World Acad Sci Eng Technol.* 2011;59:440–6.
44. Roy S, Jain V, Bajpai R, Ghosh P, Pente AS, Singh BP, Misra DS. Formation of carbon nanotube bucky paper and feasibility study for filtration at the nano and molecular scale. *J Phys Chem C.* 2012;116(35):19025–31.
45. Mahbulul IM, Saidur R, Amalina MA. Latest developments on the viscosity of nanofluids. *Int J Heat Mass Transf.* 2012;55(4):874–85.
46. O’Sullivan D, Cotterell M. Temperature measurement in single point turning. *J Mater Process Technol.* 2001;118(1–3):301–8.
47. Montgomery DC, Runger GC. *Applied statistics and probability for engineers.* New York: Wiley; 2010.